Modelling of incident sound wave propagation around sound barriers using cellular automata

doi: 10.1007/978-3-642-33350-7-40

Modelling of Incident Sound Wave Propagation around Sound Barriers using Cellular Automata

Toshihiko Komatsuzaki[1], Yoshio Iwata[1], and Shin Morishita[2]

[1] Institute of Science and Engineering, Kanazawa University, Kakuma-machi, Kanazawa, Ishikawa, 920-1192 Japan
{toshi, iwata}@t.kanazawa-u.ac.jp
[2] Graduate School of Environment and Information Sciences, Yokohama National University, 79-7 Tokiwadai, Hodogaya-ku, Yokohama 240-8501, Japan
mshin@ynu.ac.jp

Abstract. In the present study, acoustic wave propagation in the field including sound isolation panel is simulated using Cellular Automata (CA). CA is a discrete system which consists of finite state variables, arranged on a uniform grid. CA dynamics is described by a local interaction rule which is used for computation of new state of each cell from the present state at every time step. In this study a sound field is modeled using CA where the sound isolation panel exists and the numerical simulation results are evaluated quantitatively by the insertion loss. The results showed good correspondence with analytical solutions.

Keywords: Cellular Automata, Wave Propagation, Incident Sound Wave, Diffraction, Sound Barrier

1 Introduction

Not only the recent growth of roadway traffic but also the increasing number of full-sized vehicle, high-speed running cars on highways cased serious noise problems especially in urban regions. The noise abatement usually follows either the reduction of noise emitted by car itself, or the absorption and the isolation of air-borne noise within the environment. The former approach includes, for example, the development of low-noise emitting vehicle and tires. On the other hand, the latter uses noise-reducing porous asphalts and the construction of sound insulation walls beside the highways. It is physically proper that the higher sound insulation wall is preferable in order to prevent the noise leakage into the inhabited region [1], however, the high wall adversely causes some of the problems related to insolation, the landscape and also the radio disturbance. Hence the high sound insulation performance should be realized while the height of the insulation wall is kept low. The sound can be reduced by appropriately arranging the sound transmission paths along the wall shape where the sound waves are well diffracted and interfered with each other so that the outgoing sound transmission characteristic is changed. Several studies have been done for this issue devising the shape of the wall, whose noise isolation performances

are predicted analytically and numerically [2]-[6]. The development of double y-shaped noise barrier is one typical example of these works [2], where the tip of the wall consists of y-shaped branches each possessing another y-shaped sub-branches.

It is desirable that the numerical prediction of the isolation performance would be made by more efficient, precise simulation strategies. The boundary element method (BEM) is commonly used in order to predict the sound field bounded by the insulation wall, however, the method is basically suited for the stationary analysis where the harmonic sound source is assumed. Therefore, numerous calculations are required in order to obtain frequency response characteristics for a wide range of frequencies, since a harmonic response is only calculated for respective frequencies. Additionally, the expression for the moving sound source which corresponds to the sound emitted by the moving cars is hardly introduced into the BEM model. These restrictions may limit the numerical simulation to the simplified case unlike the practical situations. Another numerical method known as the finite element method (FEM) can be used, but the considerable amount of time needed for the calculation may not be negligible depending on the number of space division into elements.

The Cellular Automata has been used for modeling wide range of phenomena including many physical processes described generally by partial differential equations [7]-[10]. The authors have also developed an acoustic wave propagation model for two dimensional acoustic problems [11]. Due to its easiness and simplicity of the modeling procedure, the Cellular Automata would be suitable for representing realistic situation of the actual problems involved. In the present study, the acoustic wave propagation model constituted by Cellular Automata is applied in order to evaluate the sound isolation performance of the sound insulation wall placed within the acoustic space. The wave model is based on past studies by authors where the two dimensional acoustic problems were solved for sound source movement, diffraction, reflection and also the sound absorption. The sound isolation performance is numerically predicted for three types of insulation walls whose geometries are different: the straight wall, the wall with single y-shaped branch installed at the top, and also the wall with double y-shaped branch. As already mentioned, the third type consists of y-shaped smaller branch subordinated by the larger main y-shaped branch, where the incident sound wave and the wave traveling along the surface of the wall are interfered each other and multiply diffracted, insomuch that the dissipation of the wave energy would be expected to some extent. In order to examine the predicted results obtained by the Cellular Automata model, the calculations are also performed for the model based on boundary element method which is generally used to analyze acoustic problems. In addition, the model is compared with the theoretical model suggested by Maekawa [12], in which the insertion loss of sound energy caused by the isolation wall is predicted. It is shown that highly compatible results with other approaches can be obtained by the Cellular Automata model, while keeping the modeling procedure simple and straightforward.

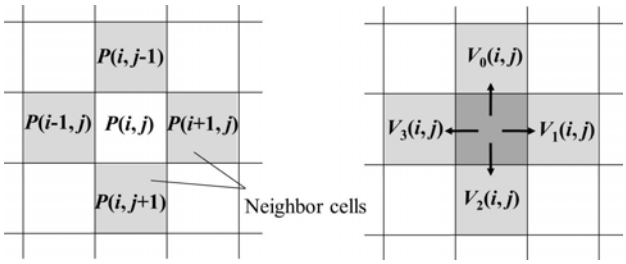

Fig. 1. Definition of neighbor in two dimensional acoustic model. Two state variables, sound pressure P and particle velocity V, are placed in each cell.

2 The Cellular Automata Model for Wave Propagation

Cellular Automata model for simulating acoustic wave propagation is shown in this section. CA has been developed for modeling wide range of phenomena including many physical processes [7]. Specifically the wave propagation models have been studied by researchers based on Cellular Automata [7]-[11]. The simple finite difference scheme obtained by linear wave equation is referenced for developing local interaction rule, in a sense that discretized wave equation yields to an expression of local relationship of wave amplitudes. The rule is then extended to a more practical case, yet time and space are treated as discrete integers. Definitions for state variables and local interaction rules are presented in the following subsections.

2.1 Space Partitioning and State Definition

Two dimensional space is discretized into rectangular cells, where state of each cell is distinguished by two integers; i) zero for acoustic media, ii) one for rigid wall. Additionally, two variables which express the sound pressure and particle velocity in four neighbor directions are defined for the acoustic medium state. These variables are updated at each simulation step according to the local interaction rules which describe the relationship between a cell and its cross-located four neighboring cells as shown in Fig.1. Following Cellular Automata convention, time and space are treated as integers. In order for the model to be comparable with actual dimension, we assign unit cell length $dx = 0.001$[m], and also $c = 344$[m/s] for the sound speed.

2.2 Definition of Local Rules

State parameters given in each cell is updated every discrete time step according to a local interaction rule. First, the particle velocities in four directions are updated in time with respect the difference of sound pressure between adjacent cells, whose update rule is described explicitly as,

$$V'_a(\mathbf{x}, t+1) = V_a(\mathbf{x}, t) - \{P(\mathbf{x} + \mathbf{dx}_a, t) - P(\mathbf{x}, t)\} \ . \tag{1}$$

V_a represents particle velocity of media and P the sound pressure. Two dimensional cell position is expressed as a vector $\mathbf{x}$ and discrete time step as t. A suffix a in (1) signifies index of four neighbors. The particle velocity further obeys the next (2), which expresses linear energy dissipation mechanism.

$$V_a(\mathbf{x}, t+1) = (1-d) \cdot V'_a(\mathbf{x}, t+1) \ . \tag{2}$$

In the above (2), d represents a damping constant per unit cell assuming sound absorption by the media. In the present study, d is given as 0.001.

The pressure is then updated according to the rule described by (3),

$$P(\mathbf{x}, t+1) = P(\mathbf{x}, t) - c_a^2 \sum_a V_a(\mathbf{x}, t+1) \ , \tag{3}$$

where c_a denotes the wave traveling speed in CA space. Sound pressure and particle velocities are updated according to the local rule described by above three equations. In addition, if the wall is totally reflective, the sound pressure values of wall state cells are copied by those of the adjacent medium state cells so that the perfect reflective condition can be represented.

Since calculation is carried out between nearby cells that are separated only a unit length at every step, any physical quantities cannot have the transport speed exceed to this calculation limit. The maximum wave speed becomes $c_a = 1/\sqrt{2}$ for two dimensional space, therefore the wave front travels $1/\sqrt{2}$ of unit length per calculation step [11].

3 Simulation of Sound Field Incorporating Isolation Wall

3.1 Description of the Model

Numerical simulation is performed for the wave propagation within two dimensional acoustic field incorporating sound isolation wall. The sound field is calculated for the simulation space of 4[m] in height and 6[m] in width, whose boundary conditions are assumed to be infinite without any reflected wave from the boundaries. Despite the easiness in realizing infinite boundary condition in BEM modeling, the finite set of cell arrangement in CA model naturally causes boundary reflection at the cells located on four edges. Therefore, the actual size of the simulation space is set as large as threefold of the analyzed space so that the reflection problem is avoided in the course of the simulation. The unit size of a cell is assumed to be 10[mm], hence the cellular space is constituted of 1200×1800 cells. A sound insulation wall is located and extended downward vertically separating the analyzed space. On the left side, the noise source is located, and the other side the sound observation points labeled by numbers from 1 to 12 are placed. The sound isolation performance is numerically predicted for three types of insulation walls whose geometries are different, as shown in Fig.3: the straight wall (type 1), the wall with single y-shaped branch installed at the top (type 2), and also the wall with double y-shaped branch (type 3). The sound

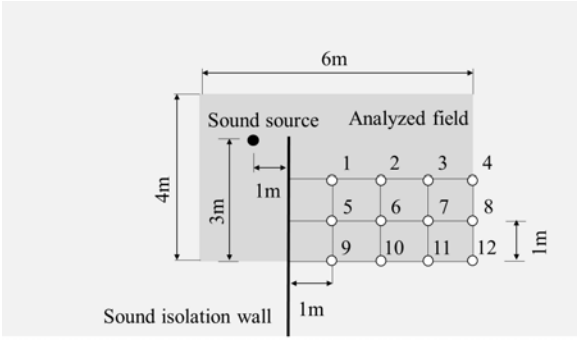

Fig. 2. Schematic of calculated sound field incorporating noise insulation wall. The numbers on grids signify the observation points of sound pressure passes over the wall.

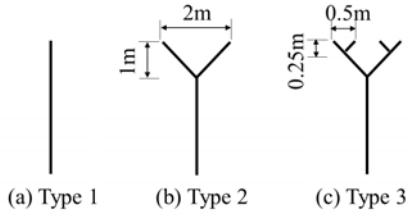

Fig. 3. Geometries of sound insulation walls.

source assuming the air-borne noise radiated by the roadway cars is placed 1[m] apart horizontally from the tip of the wall.

In both BEM and CA models, the harmonic sound source ranging from 500[Hz] to 2[kHz] at every 100[Hz] step is given and the sound pressure distribution of the field is calculated at respective frequency. Additionally, the RMS of the propagated sound pressure transmitted beyond the wall is measured at 12 points, where each pressure is normalized by the RMS reference pressure at the source location. The normalized pressure is employed as evaluation indicator when comparing the isolation performance among three types of walls. Whereas the acoustic field response analysis is rather limited to the harmonic cases in BEM model while avoiding the formulation become complex, the transient field response is easily calculated in CA model. Therefore, the random sound source response is calculated for the CA model as an additional sound source condition. By computing Fourier transformation of the observed time histories of sound pressure at measurement points and further calculate the transfer functions to the frequency characteristics at the source location, roughly the identical evaluation of the isolation performance can be made in comparison to the sinusoidal cases with just a single computation.

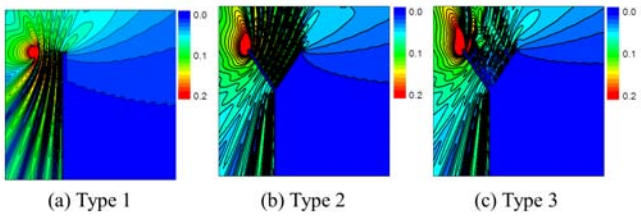

Fig. 4. Sound pressure distribution calculated by BEM for 1000Hz sinusoidal source.

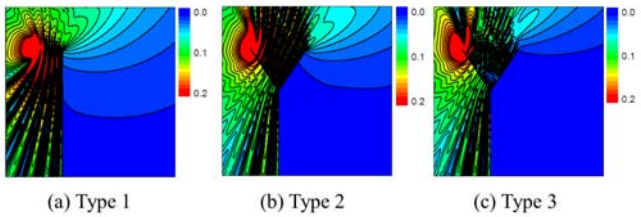

Fig. 5. Sound pressure distribution calculated by CA model for 1000Hz sinusoidal source.

3.2 Sound Pressure Distribution of the Calculated Field

Examples of calculated sound field incorporating three types of isolation walls when the sinusoidal sound source frequency is set to 1[kHz] are shown respectively for BEM and CA model in Figs.4 and 5. The sound source is located on the left side of the wall, whereas the region in which the sound transmission is undesirable is assumed to be on the right side. In each type of wall and in all the frequencies given to the sinusoidal source, approximately the consistent pressure distribution can be obtained in both models. In view of the sound isolation performance, the double y-shaped wall (type 3) mostly prevents sound transmission downward the right hand side of the wall as compared to the vertically straight type wall (type 1). The sound dissipation is thought to be occurred by the interference of the outgoing direct wave and the phase-delayed diffracted sound wave transmitting along the wall shape. These numerically predicted results are qualitatively supported by the experimental observations made by the original inventor group of double y-shaped insulation wall.

3.3 Frequency Characteristics of the Sound Isolation Performance

The measured frequency response of the sound isolation performance measured at observation points 1 and 11 are shown for three types of walls in Figs.6, 7 and 8, respectively. The calculated results are compared for sinusoidal source case in both BEM and CA models, and also for the random source case in CA model. In these figures, the insertion loss is adopted for the isolation performance evaluation, which is defined as the difference between the sound pressure level

measured at a point under the presence of the isolation wall and that without the wall. Here again it is seen that the calculation results by both models coincide well in each type of wall. What is more remarkable is that the frequency response characteristics calculated by assigning the transient sound wave in the CA model are approximately consistent with those obtained by the other two models. Despite the prediction accuracy, one could say that simulating field response of the transient sound wave incorporating multiple frequencies is useful in view of computational efficiency.

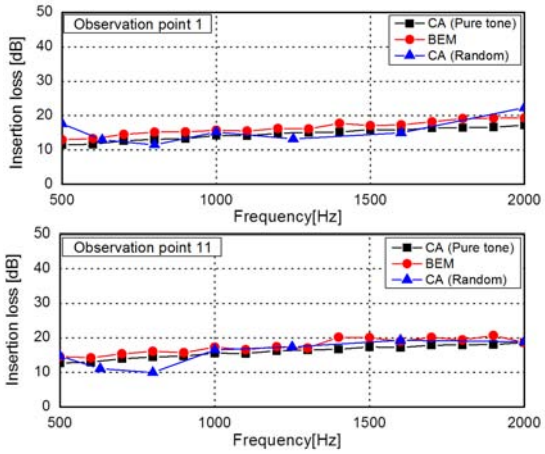

Fig. 6. Insertion loss predicted by respective calculations for type 1 wall.

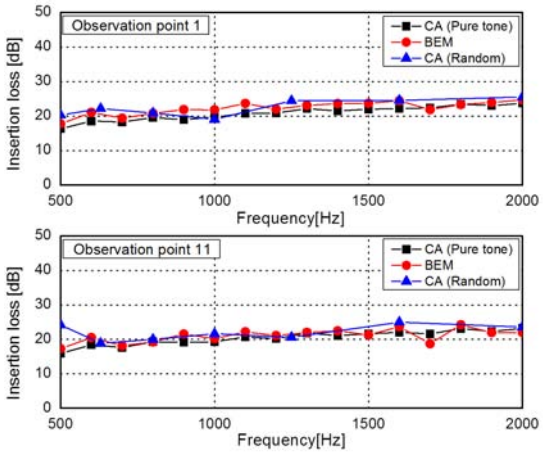

Fig. 7. Insertion loss predicted by respective calculations for type 2 wall.

In Fig.9, the insertion loss is further compared for three types of insulation walls in which the sound pressure is measured at observation point 1 and 11. The calculations are performed for the CA model where the sinusoidal sound source at respective frequency is given. It is known qualitatively from the figure that the type 3 wall shows better noise isolation performance throughout the frequency range in comparison to the other two types. Though not shown in the figure, not much difference can be seen at any other observation points.

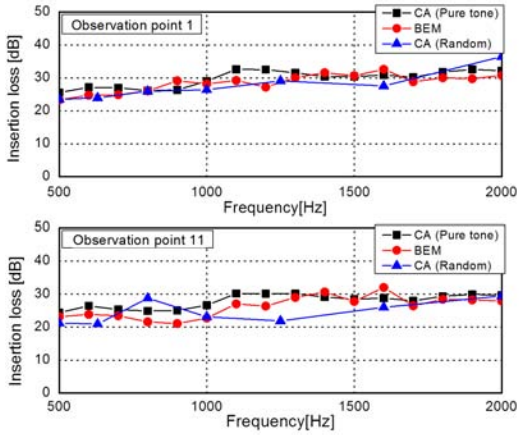

Fig. 8. Insertion loss predicted by respective calculations for type 3 wall.

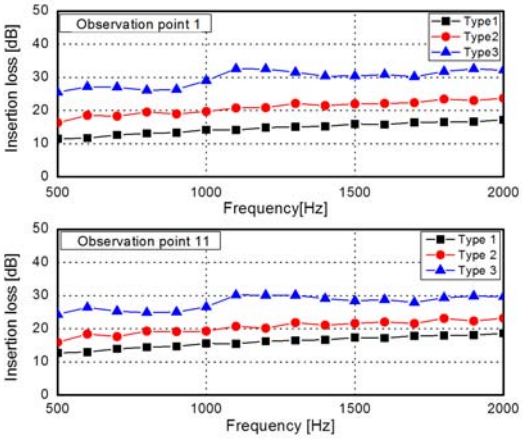

Fig. 9. Insertion loss compared by three types of walls. The measurement point is located at point 1 and 11, where the calculation results are obtained by CA model.

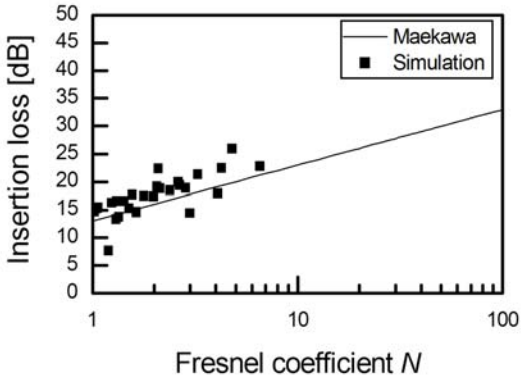

Fig. 10. Application of Maekawa's insertion loss chart to the calculated results obtained by CA simulation.

3.4 Verification of the Calculated Results using Maekawa's Insertion Loss Chart

The sound field calculated by CA model is examined based on more realistic performance criterion known as Maekawa's insertion loss chart [12]. Although limited to the straight wall case, the chart is derived from Kirchhoff's approximate diffraction theory where the formulated insertion loss is further calibrated by experimental observation. The insertion loss $[IL]$[dB] is generally plotted against Fresnel number N, defined as,

$$N = \frac{(A+B)-d}{\lambda/2} = \frac{2\delta}{\lambda} \ . \tag{4}$$

In (4), A signifies the distance between the sound source and the vertex of the wall, B the distance between the observation point and the vertex, d the straight-line distance between the source and observation points, and also λ the wavelength of harmonic sound. The Fresnel number is defined by the difference between the indirect $(A+B)$ and the direct d path of transmitted sound divided by half-wavelength of the source. The transmission loss is then represented as function of Fresnel number, which is expressed as follows.

$$\lfloor IL \rfloor_h = \begin{cases} 10\log_1 0\{N\} + 13 & N \geq 1 \\ 5 \pm \frac{8}{\sinh^{-1}} \sinh^{-1}\{|N|^{0.485}\} & -0.324 \leq N < 1 \\ 0 & N < -0.324 \end{cases} \tag{5}$$

Using the first formula for $N > 1$, Maekawa's empirical curve is shown in Fig.10 in conjunction with plots obtained by the CA model. The overall value of the plotted insertion loss exceeds the curve, one reason may be because the chart is constituted by adopting the minimum value out of empirically tested multiple data measured for each Fresnel number, based on the safe side estimation. From

the figure, the CA model shows certain level of agreement with the insertion loss criterion.

4 Conclusions

In this study, the acoustic wave propagation model is constituted by Cellular Automata and is applied to the evaluation of the isolation performance of the sound insulation wall placed within the acoustic space. The calculation results obtained by both BEM and CA models coincide well in each type of insulation wall for the harmonic sound source assumption. In addition, the frequency response characteristics calculated by assigning the transient sound wave incorporating multiple frequencies in the CA model are approximately consistent with those obtained by the other harmonic cases, which contribute to reduce computation time for the analysis. Finally, the insertion loss of the straight type wall predicted by the CA model for the straight type wall is roughly shown to be consistent with Maekawa's insertion loss criterion.

References

1. Morse, P. M. and Ingard, K. U.: Theoretical Acoustics. Princeton University Press (1986)
2. Shima, H., Watanabe, T., Mizuno, K., Iida, K., Matsumoto, K. and Nakasaki, K.: Noise reduction of a multiple edge noise barrier, Proc. of Internoise 96, pp.791–794 (1996)
3. Watts, G. R.: Acoustic Performance of a Multiple Edge Noise Barrier Profile at Motorway Sites. Applied Acoustics **47**, pp.47–66 (1996)
4. Crombie, D. H., Hothersall, D. C. and Chandler-Wilde, S. N.: Multiple-Edge Noise Barriers. Applied Acoustics **44**, pp.353–367 (1995)
5. Jin B. J., Kim H. S., Kang H. J. and Kim J. S.: Sound Diffraction by a Partially Inclined Noise Barrier. Applied Acoustics **62**, pp.1107–1121 (2001)
6. Murata, K., Nagakura, K., Kitagawa, T. and Tanaka, S.: Noise Reduction Effect of Noise Barrier for Shinkansen Based on Y-shaped Structure. QR of RTRI **47** 3, pp.162–168 (2006)
7. Chopard, B. and Droz, M.: Cellular Automata Modeling of Physical Systems. Cambridge University Press (1998)
8. Chopard, B.: A Cellular Automata Model of Large-scale Moving Objects. J. Phys. A: Math. Gen. **23**, pp.1671–1687 (1990)
9. Chen, H., Chen, S., Doolen, G., and Lee, Y. C.: Simple Lattice Gas Models for Waves. Complex Systems **2**, pp.259–267 (1988)
10. Sudo, Y. and Sparrow, V. W.: Sound Propagation Simulations Using Lattice Gas Methods. AIAA J. **33**, pp.1582–1589 (1995)
11. Komatsuzaki, T. and Iwata, Y.: Modeling of Sound Absorption by Porous Materials using Cellular Automata. Proc. of ACRI2006, LNCS, vol.4173, pp.357–366 (2006)
12. Maekawa, Z.: Noise Reduction by Screens. Applied Acoustics **1**, pp.157–173 (1968)